



Using high-frequency solute synchronies to determine simple two-end-member mixing in catchments during storm events

Nicolai Brekenfeld¹, Solenn Cotel², Mikaël Faucheux¹, Paul Floury³, Colin Fourtet², Jérôme Gaillardet⁴,
Sophie Guillon⁵, Yannick Hamon¹, Hocine Henine⁶, Patrice Petitjean⁷, Anne-Catherine Pierson-
5 Wickmann⁷, Marie-Claire Pierret², Ophélie Fovet¹

¹INRAE, Institut Agro, UMR SAS, Rennes, 35042, France

²ITES Institut Terre et Environnement de Strasbourg, CNRS/Université de Strasbourg, Strasbourg, 67000, France

³Extralab, Paris, 91400, France

⁴Université de Paris, Institut de Physique du Globe de Paris, CNRS, Paris, 75238, France

10 ⁵Centre de Géosciences, MINES ParisTech, PSL University, Fontainebleau, 77300, France

⁶University of Paris-Saclay, INRAE Jouy-en-Josas - Antony, UR HYCAR, Antony, 92761, France

⁷Géosciences Rennes UMR CNRS6118, University Rennes, Rennes, 35042, France

Correspondence to: Nicolai Brekenfeld (nicolai.brekenfeld@gmail.com) and Ophélie Fovet (ophelie.fovete@inrae.fr)

Abstract. Stream water chemistry at catchment outlets is commonly used to infer the flow paths of water through the catchment
15 and to quantify the relative contributions of various flow paths and/or end-members, especially during storm events. For this
purpose, the number and nature of these flow paths or end-members are commonly determined with principal component
analysis based on all available conservative solute data. Here, for a given pair of measured solutes, we propose a methodology
to determine the minimum number of required end-members, based on the ion's synchronous variation during storm events.
This allows identifying solute pairs, for which a simple two end-member mixing model is sufficient to explain their variation
20 during storm events and solute pairs, which show a more complex pattern, requiring a higher-order end-member mixing model.
We analysed the concentration-concentration relationships of several major ion pairs on the storm-event scale, using multi-
year, high-frequency (< 60 minutes) monitoring data from the outlet of two small (0.8 to 5 km²) French catchments with
contrasting land-use, climate and geology. A large number of storm-events (56 to 92 %) could be interpreted as the result of
the mixture of only two end-members, depending on the catchment and the ion pairs used. Even though some of these results
25 could have been expected (e.g. a two-end-member model for the Na⁺/Cl⁻ pair in a catchment close to the Atlantic coast), others
were more surprising and in contrast to previous studies. These findings might help to revise or improve the perceptual
catchment understanding of flow path or end-member contributions and of biogeochemical processes. In addition, this
methodology can identify, which solute pairs are governed by identical hydro-biogeochemical processes and which solutes are
modified by more complex and diverse processes.

30



1 Introduction

Variations of stream water solute concentrations during storm events have been studied for several decades, because of the associated large solute fluxes and their potential effect on aquatic organisms. In addition, high-frequency time series of stream water concentrations have frequently been used to characterize the event-scale hydrological and biogeochemical processes (sources, flow paths and reactions) or the ecosystem response to nutrient inputs, which are considered useful for water resources management (Bieroza et al., 2023; Hill, 1993; Rode et al., 2016). For this characterization, water isotopes, dissolved ions and other solutes serve as tracers of specific source areas, or indicators of residence times and chemical processes within the catchment. In recent decades and years, the use of auto-samplers and the development of in situ sensors, bank-side analysers and in-the-field laboratories allowed to measure an ever growing number of solutes at sub-daily to sub-hourly frequencies (Floury et al., 2017; Knapp et al., 2020; Rode et al., 2016). These high-frequency time series of the multi-elemental stream water chemistry reveal complex – and sometimes unpredictable – patterns of water sources and flow paths on intra- and inter-event scales (Knapp et al., 2020; Neal et al., 2012).

A variety of methods exist to interpret high-frequency time series of stream water chemistry. Probably the most frequently used methods are c-Q (concentration – discharge) analysis and EMMA (end-member mixing analysis), depending on the scientific or operational question and on additional available data. Without going into too much detail, event or seasonal c-Q analysis is used to infer the relative source location of the solute (proximal vs. distal) and its transport or production mechanisms within the catchment (chemostatic vs. chemodynamic, with flushing and dilution) (Evans and Davies, 1998; Godsey et al., 2009). Using the c-Q analysis, however, no direct conclusion can be drawn about the exact location of the solute sources. In contrast, the EMMA approach quantifies the contribution of identified water sources (end-members), based on the chemical signature of these sources and the assumed conservative behaviour of the solutes (Christophersen et al., 1990; Hooper et al., 1990).

The number of solutes used in EMMA studies is rarely of primary interest. Commonly, the number and identity of the water sources (end-members), whose contributions to stream flow are sought to be quantified, are known or determined based on previous knowledge of the catchment. The solutes, that differentiate those sources, are then selected in a second step (Durand and Juan Torres, 1996; Gillet et al., 2021; Ladouche et al., 2001). Alternatively, the variation in stream chemistry is used as the primary information and is subsequently used to estimate the potential end-members and their numbers (Barthold et al., 2017; Christophersen and Hooper, 1992; Hooper, 2003; James and Roulet, 2006). In this second approach, all solutes are used, that are considered to be conservatively transported within the catchment. However, using a greater number of solutes also leads to a greater number of potential end-members, that are needed to explain the observed variation in the stream (Barthold et al., 2011). Therefore, the selection of the solutes (and their number) used in an EMMA has likely important implications for the interpretations and conclusions, but is rarely discussed in detail, as mentioned by Lukens et al. (2022).

Here, we propose a new methodology to analyse high-frequency, multi-elemental time series of stream water. The proposed method relies on pairs of solutes in bivariate concentration-concentration plots (C-C plots) for storm events. These bivariate



relationships can be used to identify synchrony between two solutes during storm events. When such synchrony is observed, a two-end-member system would be sufficient to explain the variability of the two solutes in the stream. In these cases, the potential end-members can be described as a „diluted“ or „unreacted“ end-member (not to be confused with event-water) on one hand and a „concentrated“ or „reacted“ end-member on the other hand (Lukens et al., 2022). This methodology has been elaborated based on original datasets of concentration time series that are both high-frequency (23 to 45 minutes) and multi-elemental as they include all major ions. These datasets were produced by a field laboratory prototype, the so-called ‘Riverlab’ (Floury et al., 2017) installed in two observatories of the French OZCAR Critical Zone Study Network (<https://www.ozcar-ri.org>), contrasted in terms of pedo-climate and of land use and cover. The overall aim of this work is to propose a systematic methodology applicable to the analysis and interpretation of a large chemical dataset covering contrasting hydrological events from a multitude of different catchments.

2 Material, methods, and site description

2.1 Description of the study sites

High-frequency, multi-elemental analyses of stream water chemistry were conducted in two contrasting headwater catchments in France: the Kervidy-Naizin and the Strengbach catchments (Figure 1). They differ in topography (flat vs. steep), land-use (agriculture vs. forest), climate (temperate oceanic vs temperate oceanic mountainous), and geology (schist vs. granite).

2.1.1 Kervidy-Naizin

The Kervidy-Naizin catchment (5 km², ORE AgrHyS Observatory) is located in Brittany, western France (47.95° N, 2.8° W), with an elevation between 90 to 140 m a.s.l. (Fovet et al., 2018). The topography consists of gentle slopes (< 5 %). The bedrock is composed of low-permeability schists (Upper Proterozoic), overlain by fractured and fissured layers. The weathered zone is between 1 and 30 m deep and has a total porosity of 40 to 50 %. The soils (silty loams, cambisols), with a depth of 0.5 to 1.5 m, are generally well drained, except in the bottomlands, close to the streams, where hydromorphic soils (luvisols) are found. Land use is dominated by agriculture (90 % of the catchment area) associated to relatively high levels of nutrient inputs. The crop types are approximately 30 % maize, 30 % other cereals and 30 % grasslands. The cropping systems and rotations are tightly associated to the livestock type with most farms practicing pig and/or dairy farming and a few farms having no animals (Fovet et al., 2018). The climate is temperate oceanic, with average annual rainfall of 840 ± 220 mm, Penman potential evapotranspiration of 700 ± 60 mm, runoff of 330 ± 190 mm and air temperature of 11.2 ± 0.6° C (1994 to 2017). The stream frequently dries up in summer for up to several months (Fovet et al., 2018).

2.1.2 Strengbach

The Strengbach catchment (0.8 km², OHGE Observatory) is located in the Vosges Mountains, in north-eastern France (48.12° N, 7.11° E), with an elevation between 880 to 1150 m a.s.l. (Pierret et al., 2018). The topography consists of steep



slopes (20 to 30 %). The bedrock is mainly composed of Hercynian Ca²⁺-poor granite, with various levels of hydrothermal
 95 alteration and with some microgranite and gneiss outcrops. The weathered zone has a thickness of 1 to 9 m and is overlain by
 brown acidic to ochreous, coarsely grained podzols (roughly 1 m thick). Land use is dominated by planted forests (90 % of the
 catchment area), consisting of 80 % spruce and 20 % beech trees (Pierret et al., 2018). The climate is temperate oceanic
 mountainous, with average annual precipitation of 1380 mm (varying between 900 to 1710 mm), Penman potential
 evapotranspiration of 570 mm (varying between 520 to 730 mm), runoff of 760 mm (varying between 490 to 1130 mm) and
 100 air temperature of 6° C (1986 to 2015) (Pierret et al., 2018; Strohmenger et al., 2022). Snowfall occurs 2 to 4 months per year.
 The stream is fed by several intermittent and permanent springs, of which four permanent ones are used for drinking water
 supply by the nearby village. The long-term, annual runoff coefficient (runoff plus drinking water) is 0.55 to 0.60.

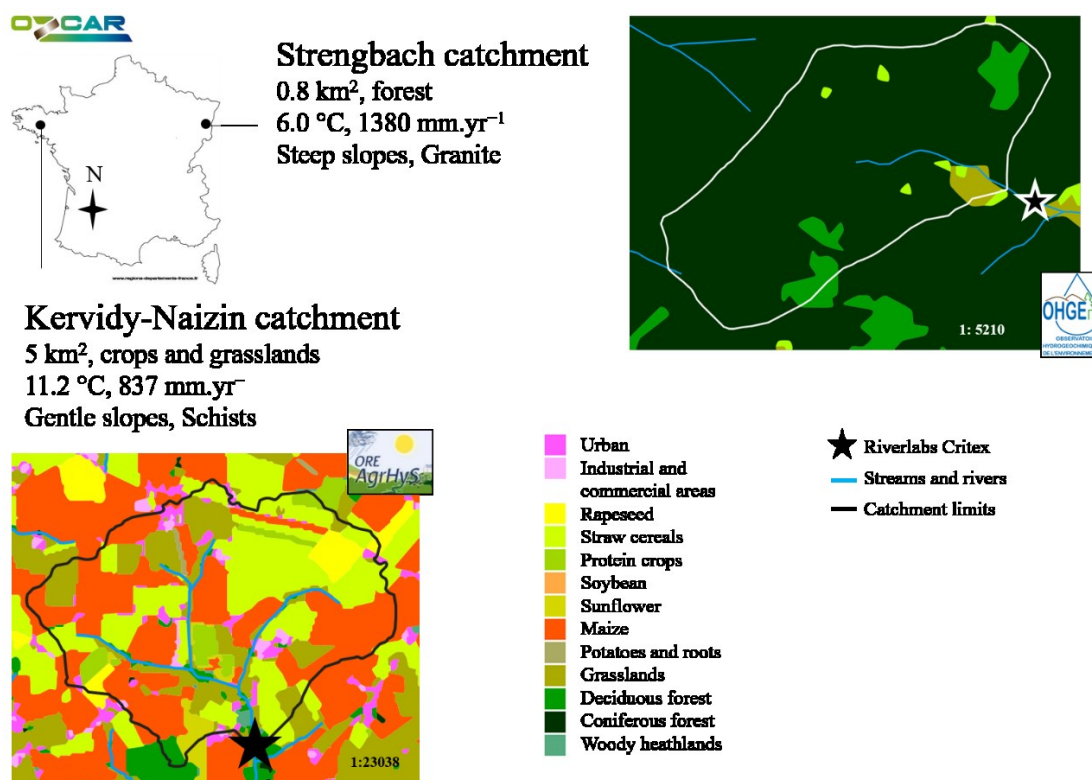


Figure 1 : Study site of Kervidy-Naizin (bottom left) and Strengbach (top right).

105 **2.2 Data acquisition**

High-frequency (every 25 to 45 minutes), multi-elemental (major cations and anions), analyses of the stream water chemistry
 at the outlets of the two catchments were achieved by automated stream-bank field laboratories. A detailed description can be
 found in Flourey et al. (2017). The two field laboratories used at the two study sites were largely identical, differing slightly
 from the original system (Flourey et al., 2017). We shortly describe here their acquisition system for the time series of the major



110 cations (Na^+ , Mg^{2+} , K^+ , Ca^{2+}) and anions (Cl^- , NO_3^- , SO_4^{2-}). It consisted of three main parts: 1.) supply of unfiltered stream water to the field laboratory, 2.) filtration and 3.) analysis of the filtered water by an ion chromatography system.

The field laboratories were located on the bank side at the outlet of the catchments. Stream water was continuously pumped by a surface pump to the field laboratory at a flow rate of around 400 to 600 l h^{-1} . The distance between the stream and the field laboratory was only a few meters (<10 m) at Kervidy-Naizin, but around 141 m at Strengbach. The mean transfer time
115 of the water from the stream to the field laboratories was equal to or less than 8 minutes (determined with salt injections).

A small fraction of the stream water was continuously filtered with a two-step filtration system. The first filtration step consisted of a stainless steel tangential filter ($0.5 \mu\text{m}$) with an automatic and regular cleaning mechanism (every few minutes), with a flow rate of roughly 0.5 to 10 l h^{-1} (depending on the site). This was followed by the second filtration step, consisting of a mixed cellulose esters membrane filter ($0.22 \mu\text{m}$), which was replaced manually weekly (Kervidy-Naizin) or biweekly
120 (Strengbach), in most cases, and with a flow rate of 0.1 l h^{-1} or less. Due to the clogging of the membrane filter and the occasional extended periods without a filter replacement (>1 week at Kervidy-Naizin and >2 weeks at Strengbach), transfer times of the filtered water to the analytical instrument reached up to 3 hours.

The filtered water was analysed by a Dionex ICS-5000 Ion Chromatography system (Thermo Scientific) for the major cations and anions every 35 to 45 minutes at Kervidy-Naizin and every 20 to 30 minutes at Strengbach. The range of time intervals
125 between two consecutive analyses at each site was due to an optimization of the analytical procedure during the course of the project. The Ion Chromatography System was calibrated, on average, monthly at Naizin and every 3 months at Strengbach and after modifications of the instrument (replacement of consumables or capillaries, etc.). Validation with standards was conducted once a month, on average. The limit of quantification was estimated to be around 1.0 mg l^{-1} for the anions and cations at Naizin as well as around 1.0 mg l^{-1} for the anions and 0.5 mg l^{-1} for the cations at Strengbach.

130 Stream discharge at both sites was estimated at the catchment outlets every minute (Kervidy-Naizin) and every 2 minutes (Strengbach) based on long-term, well-established rating curves and continuous water level monitoring.

2.3 Data treatment and analysis

The focus of this article lies on presenting a methodology to analyse and interpret the variation of the stream chemistry during storm events. We therefore only present data of storm events. The following paragraphs outline the data acquisition period as
135 well as the selection procedure of the storm events.

The field laboratories were operational from June 2018 onwards at Kervidy-Naizin and from November 2020 onwards at Strengbach. Here, we present the analysis of data collected until August 2022 in both catchments. Gaps in the dataset were due to variable technical problems, namely failure of the main pump, power cuts due to lightning, chemical alteration of the filtered water likely due to the filtration system, problems of the analytical instrument, periods without technical support and
140 the COVID-19 pandemic. To ensure reliable data quality, only periods and storm events without technical issues were selected for further analysis.



Storm events were detected semi-automatically, based on the stream discharge time series. The exact parameters and thresholds used in the procedure described below were adapted to each catchment. In a first step, the onset of a storm event was roughly detected by searching for periods of sustained, increasing stream flow, based on the first derivative of the flow. The precise starting date and time of the event, T_0 , was subsequently determined by searching for the minimum stream flow within a few hours preceding the period of sustained, increasing flow. The peak of the event was then determined with the maximum stream flow within a few days after T_0 or before the onset of the next event, whichever occurred first. The end of the event was defined by a combination of the time after the peak of the event and the stream flow relative to the initial stream flow. This event detection procedure was run automatically using an R script. All detected events were then manually verified. Finally, only storm events not impacted by the regular maintenance of the field laboratory (cleaning, calibration, filter replacement) were selected.

2.4 Development of methodology for concentration-concentration typology

2.4.1 Event-scale solute behaviour classification based on C-C plots

We propose a methodology to analyse and interpret the variation of multi-elemental stream concentrations during storm events. This methodology focuses on identifying pairs of solutes that show synchronous variations during storm events. For each possible combination of two solutes and for each event, the concentration of the first solute as a function of that of the other solute (C-C plot) was examined (Figure 2), the temporal dimension being thus lumped into the curve trajectory. We classified the observed C-C patterns into three types: 1) synchronous variation, when the two solute concentrations had a linear relationship with a coefficient of determination (R^2) larger than or equal to 0.8, 2) invariant, if at least one of the solute concentration varied by less than 10 %, relative to the initial concentration and 3) complex variation, for those cases, which could not be attributed to the first two types. Examples of each type from the two catchments are shown in Figure 2. Thus, for a given solute pair, all three variation types could be observed during different storm events.

It must be noted here that the variable and unknown transfer time of the water sample from the stream to the analytical instrument was identical for all the (seven) solutes analysed in this study (Na^+ , K^+ , Ca^{2+} , Mg^{2+} , Cl^- , NO_3^- , SO_4^{2-}), and was therefore not considered.

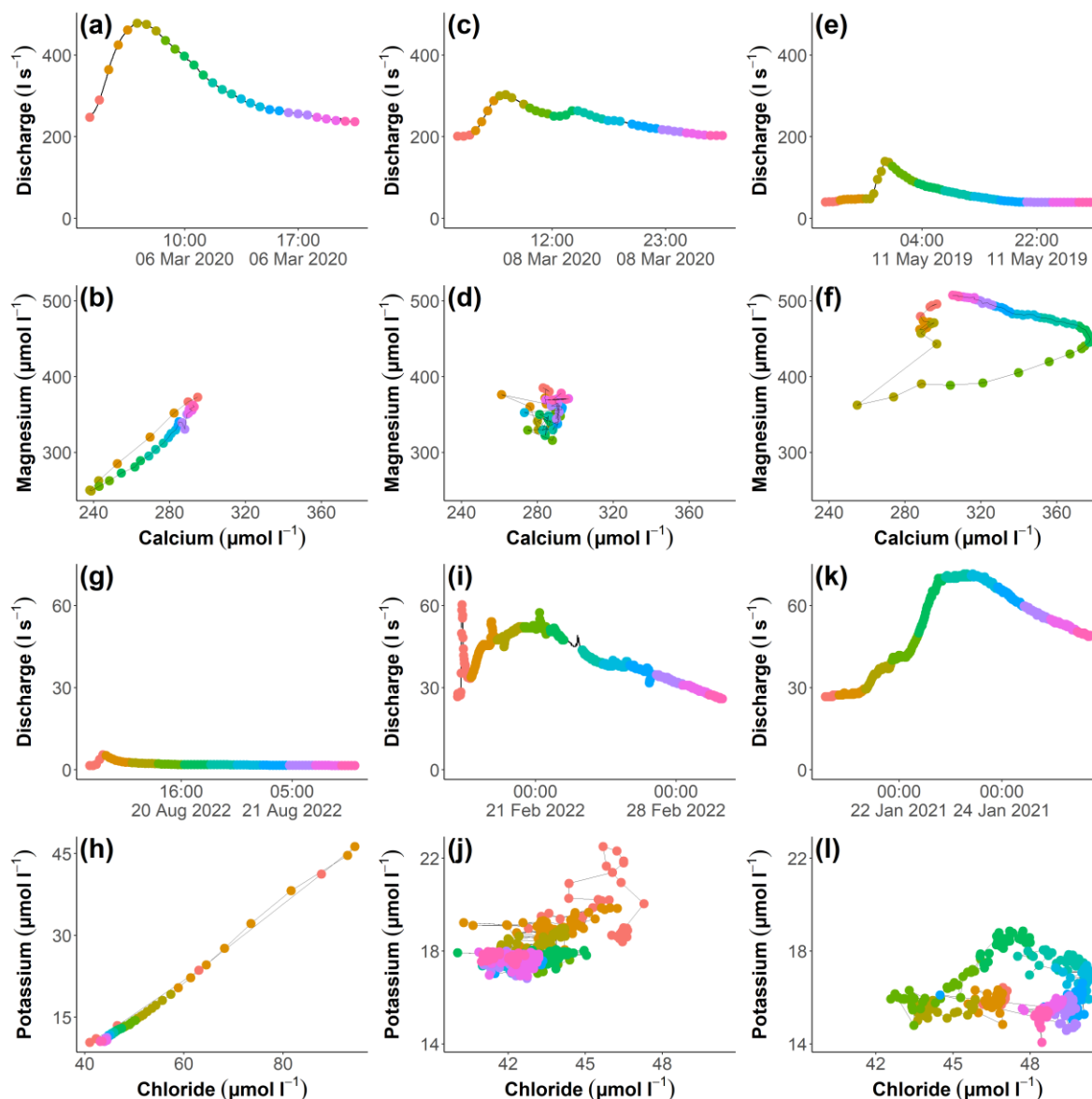


Figure 2 : Hydrographs ((a), (c), (e) & (g), (i), (k)) and the corresponding concentration-concentration plots ((b), (d), (f) for Mg^{2+}/Ca^{2+} & (h), (j), (l) for K^+/Cl^-) for three events at Kervidy-Naizin ((a) – (f)) and Strengbach ((g) – (l)). Note in the fourth row, that the scales of the axes in (h) are larger than those of the plots (j) and (l). Concentration-concentration patterns are linear ((b), (h)), invariant ((d), (j)) and complex ((f), (l)).

170

2.4.2 Rational of proposed methodology

The classification of the solutes into the three types described above provides the possibility to draw conclusions about hydrobiogeochemical processes and the activation of parts of the catchments during storm events. Synchronous solute pairs indicate that only two end-members are required to explain the variation of these solutes for a particular storm event. On a storm-event



175 scale, this could be interpreted as the mixing of one pre-event end-member, which provides baseflow, with only one event-activated end-member.

The interpretation of the solutes in the other two types (invariant and complex variation type), is more ambiguous. Invariant solutes can be interpreted either 1) as the existence of two or more end-members, which have identical chemical signatures or 2) as a flow path reactivity, that modifies and matches the concentrations of initially different end-members on their flow path
180 towards the stream. This second process was observed with a sprinkling (Anderson et al., 1997) and with a leaching experiment (Hill, 1993). Complex solutes can be caused by 1) mixing of more than two end-members, or 2) variations of the end-member concentrations during the course of a storm event.

2.4.3 Evaluation of the variation of the molar ratios on the event scale

For the synchronous solute pairs, we analysed whether and to which extent the ratio of the two solutes of the different solute
185 pairs changed during the course of individual storm events. This analysis can indicate whether the two solutes of a pair were modified by the same process(es) along the catchment flow paths towards the stream or not. For example, a constant ratio during a storm event could indicate that both solutes in the two potential end-members were modified by the same process(es) and to the same degree (e.g. increased concentrations due to evapotranspiration). However, it should be noted, that, theoretically, identical ratios in different catchment compartments/end-members could also be achieved by different processes
190 acting on the different solutes, but by chance, these different processes modified the concentrations of the two solutes to exactly the same degree. In contrast, a varying concentration ratio during the storm event indicates that both solutes in the two potential end-members were modified by different processes or to different degrees.

To evaluate the evolution of the solute ratios during the storm events, we calculated the ratio at the beginning of the storm event (the “initial ratio”) and the ratio at the time of the maximum concentration increase or decrease (the “peak ratio”). The
195 initial ratio was calculated by taking the arithmetic mean of the first two measurements during a storm event. The peak ratio was calculated as the ratio at the time, when the denominating ion (e.g., Na^+ in Cl^-/Na^+) was at its extreme value, i.e., at its minimum or at its maximum concentration.

3 Results

3.1 General chemical variation during the selected storm events

200 At Kervidy-Naizin, we selected and analysed in total 39 storm events with reliable and complete chemical data, between June 2018 and April 2022. At Strengbach, we selected and analysed 23 storm events, between November 2020 and August 2022. At both sites, the selected storm events are unevenly distributed over the experimental period, but are covering a range of discharge values in different seasons, and under different hydrological conditions. The timeline of the selected events can be seen in **Erreur ! Source du renvoi introuvable.**



205 The chemical variations during different storm events are ion- and catchment specific, and depend on the season and the hydrological conditions. Three examples are presented for each catchment in Fig. B1. On the event scale, individual ion concentrations showed contrasting evolutions: They 1) remained constant (e.g., Na^+ , Mg^{2+} , Ca^{2+} at Strengbach), 2) primarily decreased (e.g., Na^+ , Cl^- , Mg^{2+} , NO_3^- at Kervidy-Naizin), 3) primarily increased (e.g., K^+ , Cl^- at Strengbach), or 4) increased and decreased during the same event (e.g., at times Ca^{2+} or SO_4^{2-} at Kervidy-Naizin). These ion-specific patterns are either
210 consistent between events or differed from event to event, as illustrated in Fig. B1.

3.2 Event-scale concentration-concentration pattern

All three types of concentration-concentration variations were observed on the event scale. The variation type was ion- and catchment specific.

At Kervidy-Naizin, the six possible solute-pairs made of the four solutes Na^+ , Cl^- , Mg^{2+} and NO_3^- exhibited a synchronous variation pattern in over 56 % of the storm events (Table 1). This percentage was particularly high (at least 80 % of the events) for Cl^-/Na^+ and $\text{Mg}^{2+}/\text{NO}_3^-$, and lower (56 to 74 %) for the remaining four solute pairs. For Kervidy-Naizin, we will therefore refer to those four solutes as “synchronous” for the remainder of the paper.

For $\text{SO}_4^{2-}/\text{Ca}^{2+}$ at Kervidy-Naizin a synchronous variation was observed during 39 % of the storm events. The solute pairs combining SO_4^{2-} with the synchronous ions (Na^+ , Cl^- , Mg^{2+} , NO_3^-) exhibited a synchronous variation in 28 to 33 % of the storm events. This percentage was slightly lower (26 to 28 %) for the pairs made of Ca^{2+} with the synchronous ion. Potassium exhibited a synchronous variation with the other solutes during not more than 5 % of the storm events, except for Mg^{2+} (21 %) and NO_3^- (18 %). Due to these low percentages, we do not consider SO_4^{2-} , Ca^{2+} and K^+ as synchronous solutes at Kervidy-Naizin.

At Strengbach, synchronous variation during storm events were obtained only for K^+/Cl^- and $\text{Ca}^{2+}/\text{Mg}^{2+}$ (both 61 %, Table 1).
225 It should be noted, however, that this percentage was much lower (22 %) for $\text{Ca}^{2+}/\text{Mg}^{2+}$, if a threshold of 0.9 was used for the coefficient of determination (Table 1). All other possible solute pairs exhibited a synchronous variation during less than 15 % of the storm events, except for $\text{Mg}^{2+}/\text{Na}^+$ (22 %).

230 **Table 1 : Number (and percentage) of storm events with linear concentration-concentration relationships ($R^2 \geq 0.8$ or $R^2 \geq 0.9$) between different pairs of solutes for Strengbach and Kervidy-Naizin. Listed are all solute pairs that exhibit a linearity ($R^2 > 0.8$)/synchronous variation in at least 30 % of the storm events.**



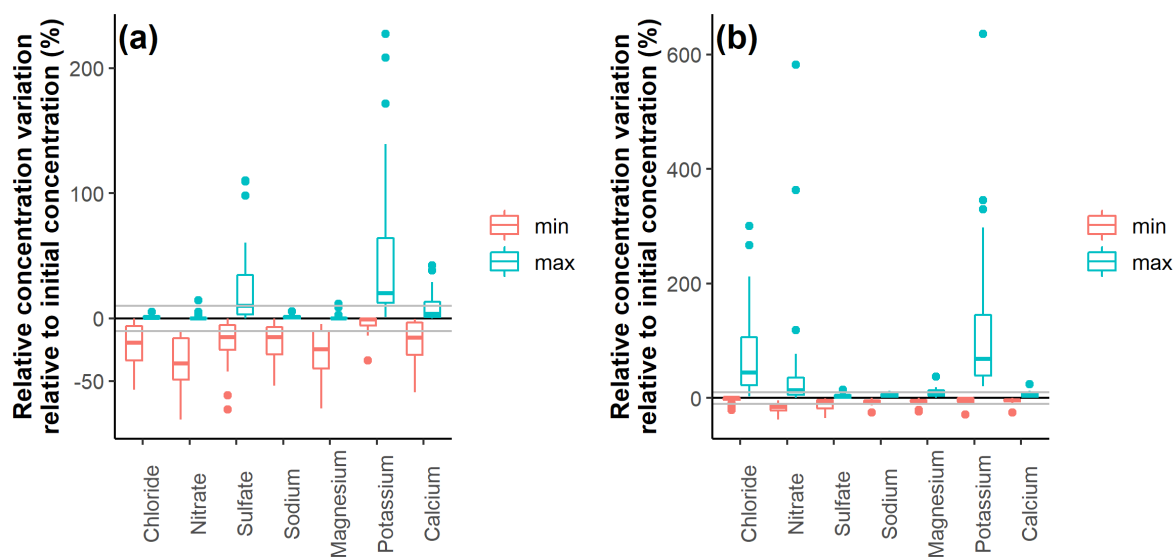
Ion Pairs	Strengbach (n = 23)		Kervidy-Naizin (n = 39)	
	R ² ≥ 0.9	R ² ≥ 0.8	R ² ≥ 0.9	R ² ≥ 0.8
K ⁺ /Cl ⁻	12 (52 %)	14 (61 %)		
Mg ²⁺ /Ca ²⁺	5 (22 %)	14 (61 %)		
Cl ⁻ /Na ⁺			31 (80 %)	36 (92 %)
NO ₃ ⁻ /Mg ²⁺			27 (69 %)	31 (80 %)
Mg ²⁺ /Cl ⁻			25 (64 %)	27 (69 %)
Mg ²⁺ /Na ⁺			24 (62 %)	29 (74 %)
NO ₃ ⁻ /Cl ⁻			20 (51 %)	24 (62 %)
NO ₃ ⁻ /Na ⁺			20 (51 %)	22 (56 %)
SO ₄ ²⁻ /Ca ²⁺			11 (28 %)	15 (39 %)
SO ₄ ²⁻ /Na ⁺			8 (21 %)	13 (33 %)
SO ₄ ²⁻ /NO ₃ ⁻			7 (18 %)	12 (31 %)

3.3 Relative concentration variations on the event scale of all solutes

235 The general event-scale variation of the different solutes is ion- and catchment-specific. At Kervidy-Naizin, consistent concentration decreases were observed on the event scale for the four synchronous ions (Na⁺, Cl⁻, Mg²⁺, NO₃⁻) for almost all events, with median concentration decreases of -15 % (Na⁺) to -36 % (NO₃⁻) (Figure 3). Consistent, event-scale mobilization patterns were observed for Cl⁻ (median: +45 %) and K⁺ (+68 %) at Strengbach, as well as for K⁺ (+20 %) at Kervidy-Naizin (Figure 3).

240 Median relative concentration variations of less than 10 % were observed for SO₄²⁻ (-8 %/+2 %; median decrease/median increase), Na⁺ (-6 %/+5 %), Mg²⁺ (-5 %/+8 %) and Ca²⁺ (-4 %/+6 %) at Strengbach. These four solutes were therefore classified as invariant solutes at Strengbach. At Kervidy-Naizin none of the solutes was classified into the invariant type (Figure 3).

245 The remaining solutes, showing a complex variation pattern, were SO₄²⁻ (-15 %/+10 %) and Ca²⁺ (-15 %/+4 %) at Kervidy-Naizin, and NO₃⁻ (-16 %/+13 %) at Strengbach. These solutes exhibited increasing and decreasing concentrations during the same event (see an example in Fig. B1) or different patterns during different events. In addition, they were not synchronous with any solute.



250 **Figure 3 : Relative concentration variation (% of initial concentration) for Kervidy-Naizin (a), n = 39 storm events) and Strengbach (b), n = 23 storm events). For each storm event i and each solute j a relative minimum (red) and a maximum (green) concentration variation C was calculated as $(C_{i,j,\min}-C_{i,j,\text{start}})/C_{i,j,\text{start}}$ and $(C_{i,j,\max}-C_{i,j,\text{start}})/C_{i,j,\text{start}}$, respectively. The grey horizontal lines indicate the 10 % thresholds. The patterns of solutes such as SO_4^{2-} and Ca^{2+} at Kervidy-Naizin (both $>10\%$ increases and decreases) are either due to some events exhibiting a primarily decreasing and others a primarily increasing concentration variation or/and due to events exhibiting both increasing and decreasing concentration variations during the same event.**

3.4 Event-scale variation of molar ratios

255 For the synchronous solute pairs, we evaluated the variation of their ratios during individual storm events. In general, the molar ratio during the events evolved towards the median ratio in the rain (at Kervidy-Naizin) or in the throughfall (at Strengbach), indicating that the ratio of the rain was closer to the ratio of the event-activated water than to the ratio of the pre-event water (e.g. baseflow) (Figure 4).

260 At Kervidy-Naizin, the relative difference between the initial and the peak ratios was small for Cl^-/Na^+ (median: -3 %) and only slightly higher for $\text{Mg}^{2+}/\text{Cl}^-$ and $\text{Mg}^{2+}/\text{Na}^+$ (median: -4 % and -7 %, respectively). In contrast, for the three pairs that include NO_3^- , the median difference between the initial and the peak ratio was larger (the medians range between -12 % and -15 %) (Figure 4). That indicates that during the storm events at Kervidy-Naizin, the relative concentration decrease was the strongest for NO_3^- , followed by Mg^{2+} , Na^+ and Cl^- .

265 At Strengbach, the ratio of K^+/Cl^- increased (median: 15 %) during the events, moving towards the ratio in the throughfall (Figure 4).

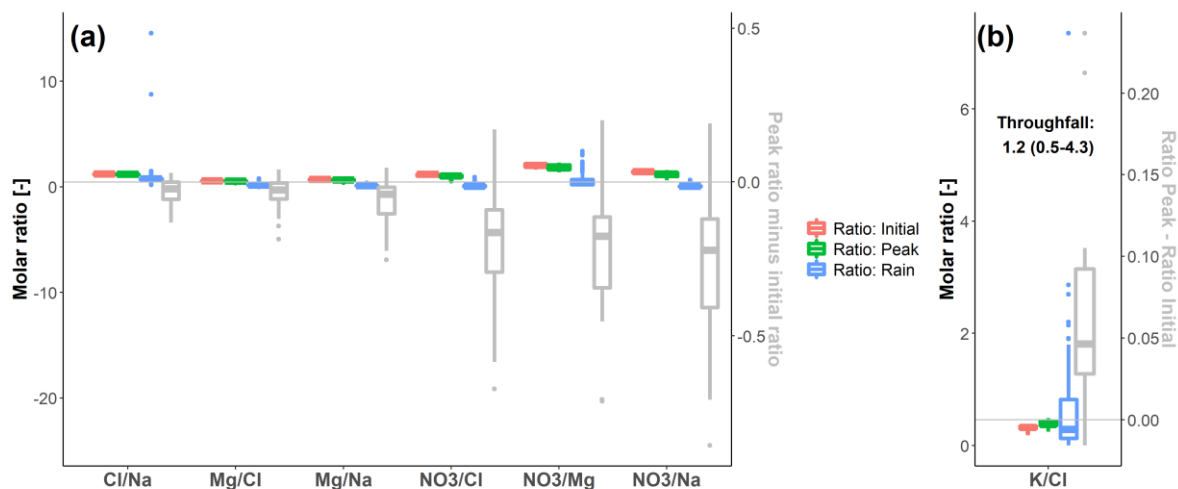


Figure 4: Concentration ratios at the beginning of the events, at the moment of the extreme value of the concentration decrease/increase („Peak“), their pairwise difference (grey) and the ratio in the rain (blue), for Kervidy-Naizin (a) and Strengbach (b). For Strengbach, the median and interquartile-range are additionally given for the throughfall. Ratios are only calculated for the synchronous solute pairs and for those events for which synchronous variations were observed for the specific ion pair.

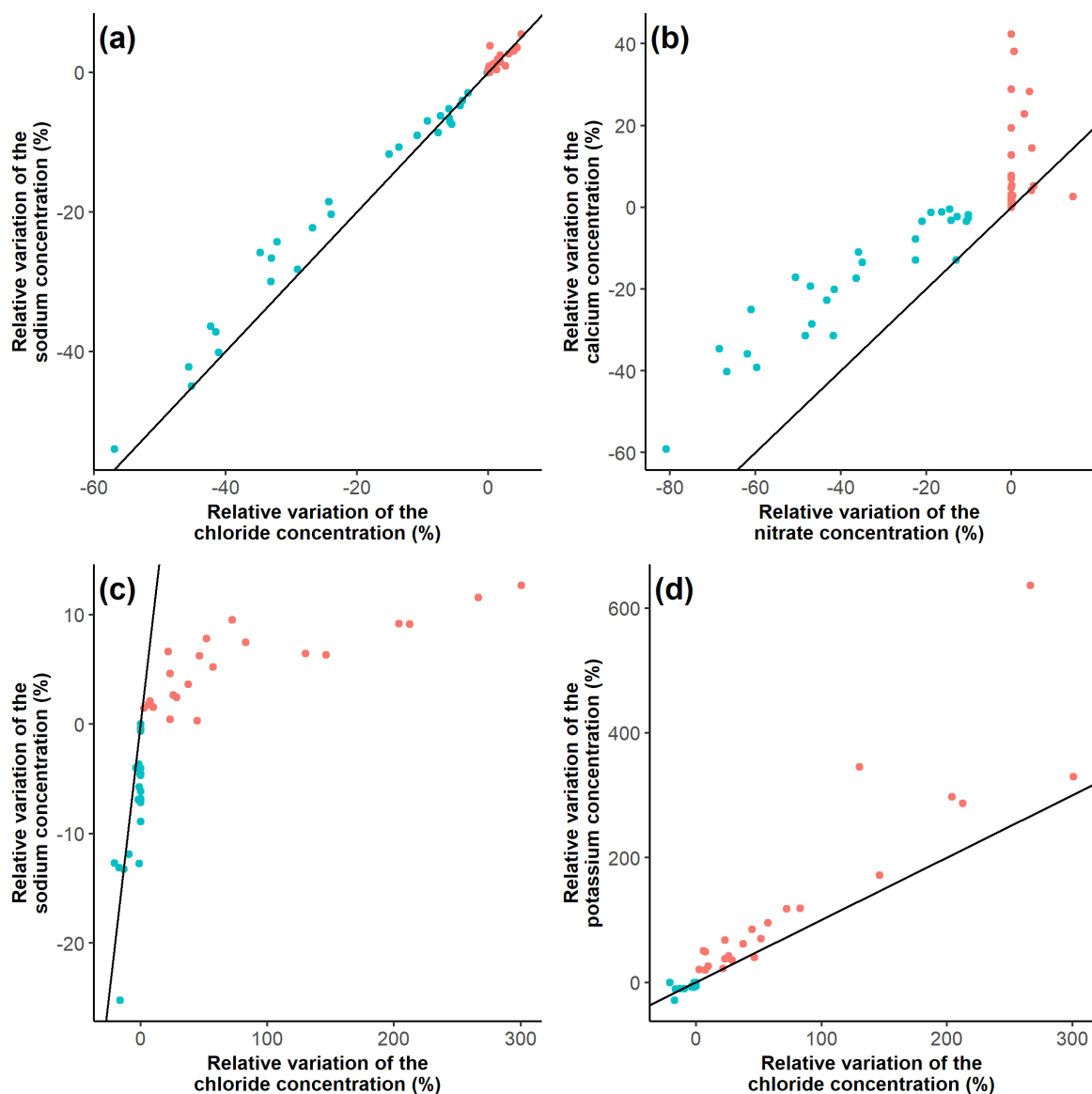
3.5 Inter-event synchrony of concentration variations

The inter-event synchrony of a solute pair compares the concentration decrease and increase of one solute across all analysed storm events with the inter-event concentration decrease and increase of another solute. This method allows evaluating, for example, whether, during a particular storm event, a minor concentration decrease of one solute also leads to a minor concentration decrease of another solute, and whether this correlation is observed across different storm events. For this purpose, we used the relative concentration variations as in Figure 3. For each storm event i and for each ion j , we calculated minimum and maximum concentration changes, relative to the initial concentrations at the start of the storm events ($C_{i,j,min}-C_{i,j,start}$)/ $C_{i,j,start}$ and ($C_{i,j,max}-C_{i,j,start}$)/ $C_{i,j,start}$, respectively.

The solute pairs that were synchronous on the event scale (Na^+ , Cl^- , Mg^{2+} and NO_3^- at Kervidy-Naizin; K^+/Cl^- at Strengbach) were also synchronous on the inter-event scale. Some examples are shown in Figure 5, for the rest see Fig. C1 and C2.

At Kervidy-Naizin, the inter-event correlation coefficients for all six pairs of the four synchronous solutes was >0.9 , indicating a strong inter-event synchrony. Ca^{2+} and SO_4^{2-} (solutes with a complex variation pattern on the event scale) showed synchrony with the other synchronous ions for those events (or parts of events), which were *diluting*: The correlation coefficients of Ca^{2+} with the four synchronous ions ranged between 0.86 and 0.93 (Fig. C1) and those of SO_4^{2-} ranged between 0.59 and 0.69 (Fig. C1).

At Strengbach, the inter-event correlation coefficient of the synchronous solute pair (K^+/Cl^-) was 0.93 (Figure 5 and Fig. C2), indicating a high synchrony on the inter-event scale. The inter-event correlation coefficients of the invariant solutes (Mg^{2+} , Ca^{2+} , Na^+ , SO_4^{2-}) ranged between 0.82 and 0.88, except for $\text{Mg}^{2+}/\text{Ca}^{2+}$ (0.96) (Fig. C2), equally indicating some degree of inter-event synchrony.



290

Figure 5 : Inter-event synchrony for Na^+/Cl^- and $\text{Ca}^{2+}/\text{NO}_3^-$ at Kervidy-Naizin ((a) and (b), respectively) and for Na^+/Cl^- and K^+/Cl^- at Strengbach ((c) and (d), respectively), as examples. All remaining pairs are visualized in Fig. C1 and C2. Relative concentration increase [red: $(C_{\text{maximum},j} - C_{\text{initial},j}) / C_{\text{initial},j}$] and decrease [green-blue: $(C_{\text{initial},j} - C_{\text{minimum},j}) / C_{\text{initial},j}$] of each event j in (%), in relation to the initial concentration. Two points therefore represent each event: the minimum (green-blue) and the maximum (red) relative concentration. The black line is the 1:1 line.

295



4 Discussion

4.1 Synchronous solute variation on the event scale

The synchronous variation of two solutes on the event scale can be interpreted as a mix between only two end-members: one “reacted”/“concentrated” and one “unreacted”/“diluted” end-member (Lukens et al., 2022). The aim is not to identify the
300 different end-members, but rather to conclude that only two different end-members are contributing to stream flow. However, at a later stage, these theoretical end-members can be mapped to some water masses.

These two end-members can be interpreted as one pre-event end-member, which is providing stream flow before and during the storm event, and one event-activated end-member. The fact that only one event-activated end-member exists for a given solute pair, indicates that the different parts of the catchment that are activated during the storm event, all have an equivalent
305 chemical signature and are spatially homogeneous without chemical “hot-spots”. Therefore, also the processes are spatially homogeneous, that are leading to the “reacted”/“concentrated” and “unreacted”/“diluted” end-members. These processes could be wet and dry deposition, evapotranspiration, weathering of primary minerals, formation and dissolution of secondary minerals, anthropogenic inputs and biogeochemical transformations, to name only a few.

4.1.1 Agricultural catchment

310 At Kervidy-Naizin, the Na^+/Cl^- ratio measured in the stream, in piezometers, or in soil solutions is very similar to and overlapping with the ratio in the rain. We, therefore, interpret that evapotranspiration is the primary process leading to the elevated solute concentration in the “concentrated” end-member, which is in line with some previous interpretations from the same catchment (Ayraud et al., 2008), and that inputs from anthropogenic activity (Cl^-) or weathering (Na^+) are negligible compared to the input from precipitation. The apparent negligible anthropogenic input of Cl^- is in contrast to interpretations of
315 previous studies from the same catchment, where inputs of mineral KCl fertilizers by the farmers were hypothesized (Aubert et al., 2013). This is similar for Na^+ , for which an input from weathering and soil leaching to the stream export was expected at Kervidy-Naizin. In a similar, granitic bedrock, agricultural catchment in Brittany, a weathering input of over 50 % was estimated for Na^+ (Pierson-Wickmann et al., 2009) and increased Na^+ concentrations and Na^+/Cl^- ratios were observed across different rivers in Brittany over the last decades, likely due to NH_4 oxidation induced acidification and soil leaching (Aquilina
320 et al., 2012). Based on these studies, the observed negligible inputs of Cl^- and Na^+ from agricultural inputs and weathering, respectively, were unexpected. This is in contrast to the Strengbach catchment, where the Na^+ input by rainwater is less important and which in turn increases the importance of the input by weathering (Ackerer et al., 2020; Pierret et al., 2014).

At Kervidy-Naizin, the stream water ratios of Mg^{2+} and NO_3^- with the other synchronous ions is elevated compared to the rain ratios. The $\text{Mg}^{2+}/\text{Cl}^-$ and $\text{Mg}^{2+}/\text{Na}^+$ ratios in the stream and piezometers are around 5 times higher than in the rain, whereas the
325 ratios of those solutes (Mg^{2+} , Cl^- , Na^+) with NO_3^- are even higher (ten times higher in the case of Na^+ and Cl^- ; 2 times higher for Mg^{2+}). This indicates that there must be additional inputs of Mg^{2+} and NO_3^- due to weathering, soil leaching, liming and/or (chemical) fertilizer applications, relative to Na^+ and Cl^- . This was expected especially for NO_3^- due to the strong agricultural



activity in the catchment. For Mg^{2+} , an input due to soil leaching and weathering could have been expected as well, based on previous observations in Brittany (Aquilina et al., 2012; Pierson-Wickmann et al., 2009). From the observed synchrony
330 between those solutes, which indicates a two-end-member system, we can conclude 1) that the inputs must be spatially homogeneous in order to lead to a two-end-member system and 2) that there are no hot-spots within the event-activated parts of the catchment, such as wetlands stimulating denitrification, that would retain or mobilize Mg^{2+} or NO_3^- differently. For NO_3^- , for example, this indicates that the impact of potential hotspots of denitrification is likely negligible for the stream chemistry during storm events.

335 The observation that the ratios of ion pairs evolve towards the lower ratios in the rain during storm events, indicates either a partial dilution by rainwater or an activation of an end-member, where the biogeochemical reactions have not proceeded as far as in the reacted/concentrated end-member. In the latter case, that means the concentrations of NO_3^- and Mg^{2+} relative to Na^+ and Cl^- are lower than in the concentrated end-member. This could be expected for Mg^{2+} , for which a significant input by rock weathering is assumed. For NO_3^- , with a larger agricultural input, this might seem to be less evident. However, it could indicate
340 the importance of the large legacy effect of NO_3^- in the deep groundwater, leading to a relatively higher concentration in the concentrated/reacted end-member (Molénat et al., 2002) or a relatively reduced concentration in the un-reacted/event-activated end-member due to denitrification.

4.1.2 Forested catchment

At Strengbach, K^+/Cl^- is the only synchronous solute pair, which can be explained by a preserved signal from throughfall.
345 Particularly high concentrations and fluxes of K^+ in throughfall (average of 31.6 and 22.4 $kg\ ha^{-1}\ y^{-1}$ under beech and spruce plots, respectively), relative to rain (2.2 $kg\ ha^{-1}\ y^{-1}$) and the export at the catchments outlet (5.5 $kg\ ha^{-1}\ y^{-1}$), were observed in this catchment and were interpreted as an input from biological excretion of leaves (Pierret et al., 2019). In addition, K is the only chemical element whose fluxes and concentrations at the outlet at Strengbach are lower than its inputs (atmospheric plus throughfall), indicating the minor importance of the weathering fluxes and a strong biogeochemical cycling in the forest.

350 Similarly, but in smaller proportions, higher inputs of Cl^- were also observed under beech (13 $kg\ ha^{-1}\ y^{-1}$) and spruce trees (19 $kg\ ha^{-1}\ y^{-1}$), in comparison with rain (6.4 $kg\ ha^{-1}\ y^{-1}$), due to the dry interception by the leaves and needles (Pierret et al., 2019). As no identified minerals from the soils and the granite contain Cl^- , the weathering fluxes of Cl^- is considered negligible at Strengbach. We therefore hypothesise, that the synchronous K^+ and Cl^- peaks during storm events might be due to higher contributions of superficial fluxes strongly influenced by throughfall. Due to the large flux from throughfall, its signal might
355 be observable in the stream. However, on its path to the stream, some of the K^+ ions are probably retained by vegetation or mineral surfaces, because the K^+/Cl^- ratio in the stream and the tributaries is close to the ratio in the rain, and lower than in the throughfall. This is underpinned by a study in the catchment that indicate, that soil solutions show a reduction in the K^+ concentration with depth (factor of almost five between 5 and 60 cm depth) (Beaulieu et al., 2020), highlighting the strong recycling by the vegetation.



360 Similar observations (increasing K^+ and Cl^- concentrations during storm events) were also reported from a small (4 ha), steep, forested catchment on low-grade metamorphic schist with a mountainous Mediterranean climate in northern Spain (Ávila et al., 1992). The authors attributed the low K^+ concentrations during baseflow to uptake by the vegetation and fixation into clay lattices and the increased storm event concentrations to mobilization from the canopy and the organic soil layer (Ávila et al., 1992), which might be applicable here, too. However, despite the fact that the authors did not use the concentration-
365 concentration behaviour of K^+/Cl^- to analyse their synchrony, as we propose here, the behaviour of K^+ and Cl^- seems to be visually less synchronous than what we observed at Strengbach. An increasing, or variable, K^+ concentration behaviour during storm events was also reported from other steep, forested catchments and was attributed to a mobilization from live or dead biomass or cation exchange buffering in the soil layer (Barthold et al., 2017; Knapp et al., 2020). However, to our knowledge, the largely synchronous behaviour of K^+ and Cl^- , which we observed at Strengbach and which indicates a two-end-member
370 system, was not reported previously and was unexpected for us.

The synchronous behaviour of Mg^{2+}/Ca^{2+} concerned only 22 % of the storm events with a threshold of the coefficient of determination of 0.9, but 61 % with 0.8 (Table 1). This correlation can be explained by their similar chemical properties and characteristics concerning the biological uptake, cationic exchange, atmospheric deposition, or soil and bedrock weathering (Pierret et al., 2014).

375 4.2 Inter-event scale synchrony

The inter-event synchrony evaluates whether different solute pairs show a similar behaviour and intensity of their concentration decreases and/or increases across different storm events. For example, at Kervidy-Naizin, Cl^- and Na^+ are synchronous on the inter-event scale: during small storm events, for example, when Cl^- is diluted by 20 %, Na^+ is also diluted by 20 %, and during large storm events both are diluted by up to 60 %. This 1:1 dilution behaviour for Cl^- and Na^+ agrees with the observation, that
380 their ratio remains almost constant during individual events. Other solute pairs, such as Cl^- and NO_3^- are synchronous on the inter-event scale, but they do not lie on the 1:1 line, because their ratio varies during individual storm events.

The observed inter-event synchrony of the synchronous ions in both catchments indicates that similar processes do not only govern these solutes during individual storm events but also across different events. Consistent variation patterns across different storm events for specific groups of ions were observed previously (Ávila et al., 1992). Storm events showing a strong
385 concentration increase (at Strengbach) or decrease (at Kervidy-Naizin) of the synchronous ions can then either be interpreted as a large contribution of the event-activated end-member or as a chemistry of the event-activated end-member that changed relative to previous storm events. Changes in end-member chemistry, linked to antecedent hydrological conditions, season or microbial activities (Knapp et al., 2020), and variable end-member contributions across different storm events (Pierret et al., 2014) were also observed before. Overall, synchronous ions on the event scale and on the inter-event scale indicate that the
390 hydro-biogeochemical processes, that lead to the diluted and concentrated end-members, are common for those ions.



4.3 Limitations of the proposed methodology

The proposed methodology for analysing high-frequency stream chemistry data is based on event-scale variations of the concentration of different solute pairs (concentration-concentration variations). We propose this methodology, because it can add useful information to those gained from other methodologies commonly used (such as EMMA, or cQ-analysis). However, it also has its limits, especially 1) the criteria used to define the different solute types and 2) the difficulty to interpret solutes with a complex and invariant variation type.

4.3.1 Sensitivity of the classification

We used the coefficient of determination of the linear regression of the concentration-concentration variation of a solute pair to define a synchronous variation and, more specifically, a threshold of 0.8. Certainly, other thresholds and linearity criteria could be used. We believe that a threshold of 0.8 is a good compromise between misidentifying complex solutes as synchronous ones and disregarding synchronous solute pairs, which are noisy due to technical uncertainties. In addition, slightly non-linear concentration-concentration variations, which could be caused by a small contribution of a third end-member, are likely classified into the synchronous variation type, when using the 0.8 coefficient of determination threshold.

The three proposed types of solute variation (synchronous, complex, invariant) are potentially overlapping and not fully mutually exclusive. For example, we observed at Strengbach for $\text{Ca}^{2+}/\text{Mg}^{2+}$ that their concentrations vary synchronously in a large percentage of storm events. However, their relative variation remains commonly below 10 %. These characteristics allow Ca^{2+} and Mg^{2+} to be grouped into the synchronous and the invariant type. Here, we grouped them into the invariant type, even though processes leading to the two variation types (two end-member system, flow path reactivity) could be considered together for their interpretation.

4.3.2 Difficulties to interpret complex solute variations on the event scale

A complex solute variation pattern is not easily to interpret, as it may be caused by several different processes, which cannot be distinguished with the method proposed here. Some of these explaining processes are 1) mixing of at least three chemically different end-members, 2) intra-event variations of the end-member concentrations of a two-end-member system and 3) non-linear reactions along the flow path between the “source” of the end-member and the stream.

The complex solutes at Kervidy-Naizin (SO_4^{2-} , Ca^{2+} , K^+) are the solutes with the lowest molar baseflow concentrations ($\leq 300 \mu\text{M}$) of the seven solutes analysed and are influenced by a strong biological activity (Beaulieu et al., 2020; Cenki-Tok et al., 2009; Pierret et al., 2019). Therefore, spatially or temporally varying processes and reactions might gain in importance, relative to simple dilution and might therefore lead to complex variation patterns. Potassium, as the solute with the lowest baseflow concentration, showed almost exclusively increasing concentrations during storm events, which were not in synchrony with any other analysed solute. These complex variation patterns of K^+ might be linked to its strong cycling in the vegetation and its mobilization from live or dead organic matter in the soil (Barthold et al., 2017; Knapp et al., 2020), including



leaching from soils after fertilizer applications. At Strengbach, NO_3^- was the only solute with a complex variation pattern, with increasing and decreasing concentration patterns during different storm events. In this catchment, NO_3^- shows the strongest annual variation, due to concentration variations in the different sources and their variable relative contributions during the year. These observations might explain the complex event-scale variation pattern of NO_3^- at Strengbach. However, this was in contrast to the strong concentration decreases of NO_3^- observed at Kervidy-Naizin, where, due to the agricultural activities, the baseflow concentrations were 20 to 50 times higher than at Strengbach. However, in other forested headwater catchments with baseflow concentrations similar to those at Strengbach, complex variations of NO_3^- were also observed and were interpreted as supply limited leaching of NO_3^- from organic soil layers or variable biological uptake (Ávila et al., 1992; Knapp et al., 2020).

4.3.3 Difficulties to interpret invariant solutes on the event scale

At Strengbach, we observed, that the majority of the analysed solutes exhibited no or only a limited concentration variation during storm events (Ca^{2+} , Mg^{2+} , Na^+ , SO_4^{2-}). As mentioned above, this can be caused by various different processes. In addition, this limited concentration variation could mean that these solutes are not relevant to infer event-scale processes but it could also be related to the characteristics of the analysed events.

Another limitation of our analyses relates to the selection of analysed storm events. Due to technical challenges (pump failure, filter clogging, power outages due to lightning strikes) specifically large storm events were not analysed by the field laboratories at both sites. Therefore, the analysed storm events, which we presented in this article, probably do not represent all possible storm events and their effects on the stream chemistry, but are likely biased towards small to medium intensity storm events.

4.4 Advantage of the proposed methodology and difference to other methods

The advantage of the proposed methodology lies in its very simple application and the additional information gained when analysing high-frequency multi-elemental stream chemistry data during storm events. It can provide information about solute specific processes in catchments without requiring a priori assumptions. For example, our methodology requires much less prior knowledge of the catchment processes than the classical EMMA approach (Durand and Juan Torres, 1996). In addition, our methodology does not require the a priori assumption of conservative solutes, as it is required in the EMMA approach (Christophersen et al., 1990).

In comparison to the multi-variate analysis based on the principal component analysis, which provides the number of potential end-members using the ensemble of all “conservative” solutes (Christophersen and Hooper, 1992; Hooper, 2003), the methodology proposed here evaluates the potential number of end-members for pairs of different solutes. This has two advantages. Firstly, a greater number of solutes used in the PCA analysis also leads to a greater number of potential end-members, which are required to explain their total variation (Barthold et al., 2011). It is therefore not straightforward to know which, and specifically how many solutes should be used in the PCA, because both might have a large impact on the outcome



of the analysis (i.e., the number of potential end-members). In the methodology proposed here, this ambiguity is removed.
455 Secondly, based on the PCA, it is not straightforward to know which solutes are responsible for a higher-order mixing model
and for which solutes a simpler model would be sufficient. Again, the methodology proposed here allows distinguishing the
synchronous solutes that are governed by similar processes, from those, which are associated to more complex variation
patterns, likely due to additional solute specific processes.

5 Conclusion

460 In this study, we presented high-frequency stream chemistry data collected with an innovative infrastructure (Riverlab) that
enabled us to sample systematically a large number of flood events, more than what is frequently collected with an automatic
sampling strategy. Based on these high-frequency, multi-elemental timeseries of stream solute concentrations, we propose a
complementary methodology, which allows identifying solutes that are governed by mixing only two end-members during
storm events.

465 The proposed methodology is based on using concentration-concentration variations during storm events (i.e., the variations
of the concentrations of solutes A and B against each other) to identify synchronous solute pairs. Those synchronous solutes
can be interpreted as mixing of only two end-members: one concentrated/reacted end-member and one diluted/unreacted end-
member. This two end-member system can also be viewed as consisting of one pre-event and only one event-activated end-
member. The concentrations of the synchronous solutes are thus spatially homogeneous in the catchment, without significant
470 alteration in hotspots . Alternatively, the contributions from those hot-spots are negligible during storm events.

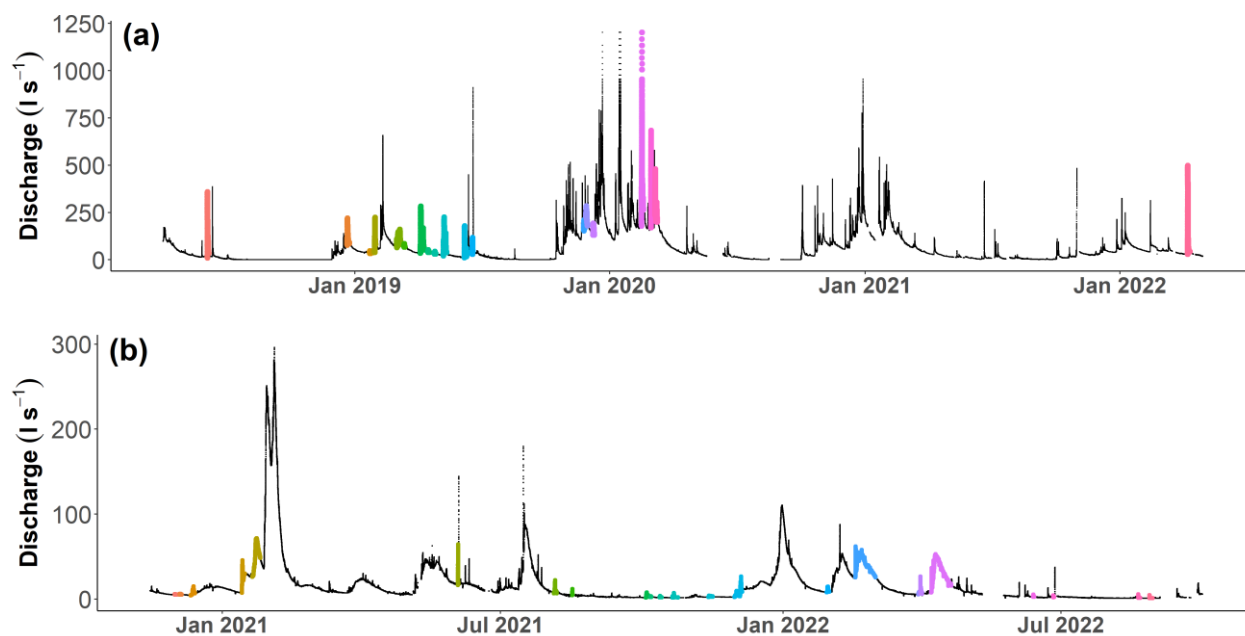
We observed a synchronous concentration variation of four solutes (Na^+ , Cl^- , Mg^{2+} , NO_3^-) during 56 to 92 % of the analysed
storm events at the agricultural catchment (Kervidiy-Naizin) and for two solutes (K^+/Cl^-) during 61 % of the storm events at
the forested catchment (Strengbach). Therefore, these solutes are governed by only two end-members during the majority of
the storm events. Even though a synchronous concentration variation could have been expected for some of these solutes, it
475 was unexpected for the majority of them.

These results show the potential impact of land cover, geology, topography and climate on the relation between the stream
water chemistry and the hydrological dynamic. For example, the absence of fertilizers and soils modified by agriculture at
Strengbach, in contrast to Kervidiy-Naizin, might be one of the reasons why no common pairs of synchronous ions were found
between the two studied sites. Thus, land cover and human activities modify the hydrological dynamics as well as the
480 geochemical signatures.



Appendices

Appendix A: Hydrographs of Kervidy-Naizin and Strengbach with the selected storm events



485 Figure A1: Hydrograph with selected and analysed storm events (colored) for Kervidy-Naizin (a) and Strengbach (b).



Appendix B: Examples of the chemical variation of the stream water during storm events

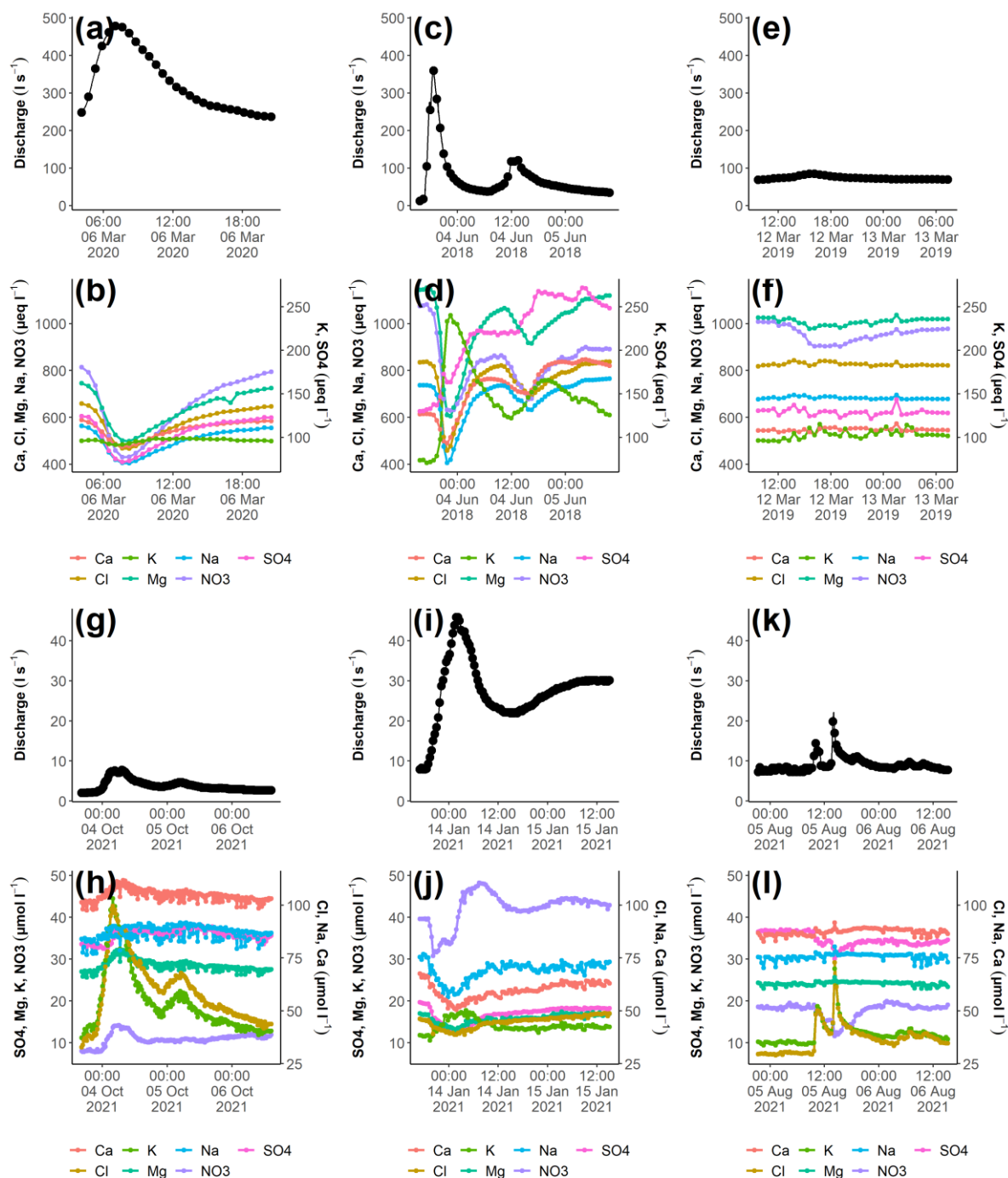
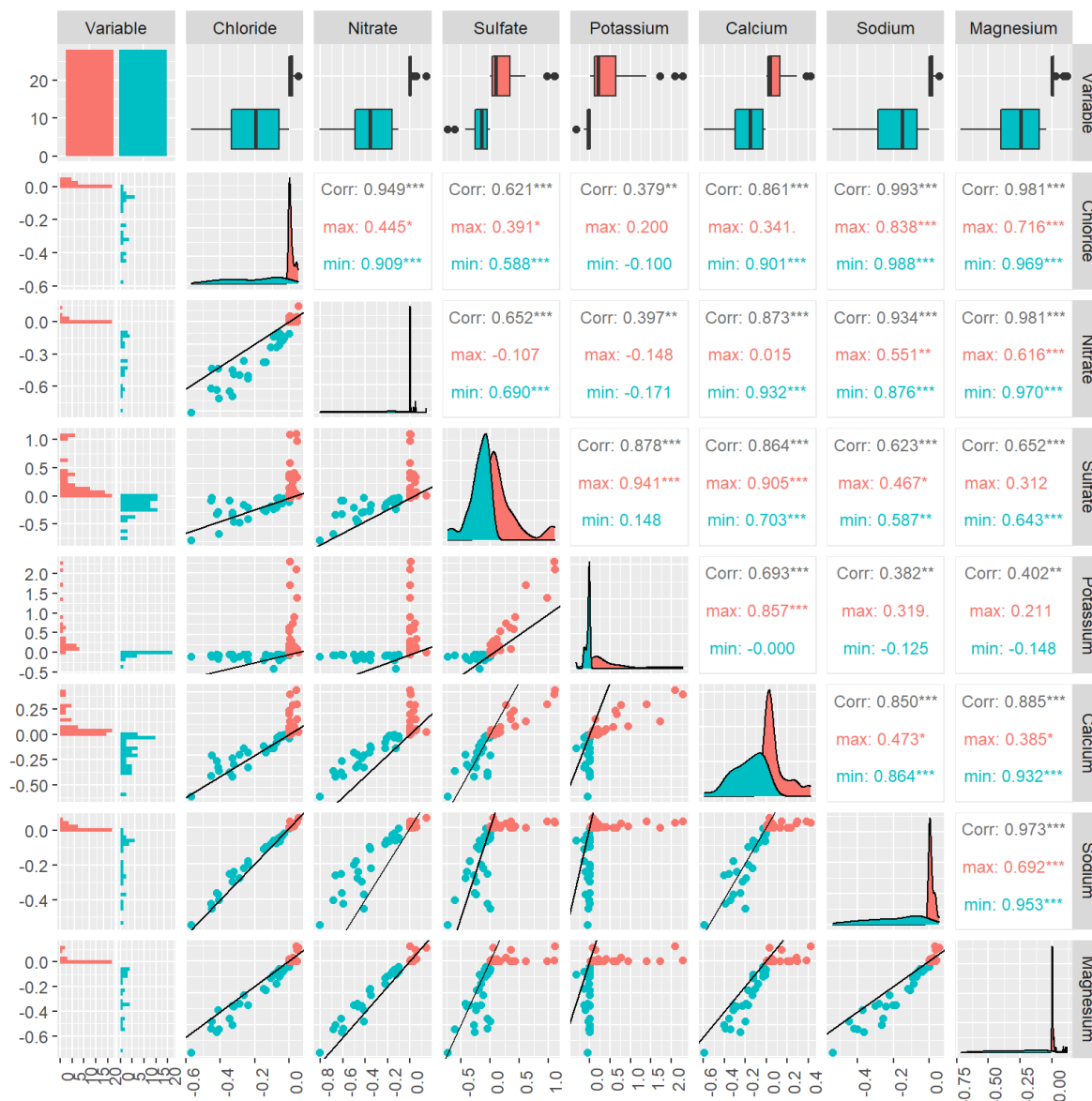


Figure B1: Examples of the chemical variation during three different storm events at Kervidy-Naizin ((a) – (f)) and Strengbach ((g) – (l)). For each storm event, the discharge ((a), (c), (e) & (g), (i), (k)) and the corresponding chemical concentrations ((b), (d), (f) & (h), (j), (l)).



490 (h), (j), (l) are visualized. In order to highlight the inter-event variability, the y-axes for the discharge and the chemical concentrations are held constant for each catchment.

Appendix C: Inter-event synchrony for all solute pairs



495 **Figure C1: Inter-event synchrony for all 21 solute pairs for Kervidy-Naizin. Lower-left triangle of sub-figures : Relative concentration increase [red; $(C_{\text{maximum}, j} - C_{\text{initial}, j})/C_{\text{initial}, j}$] and decrease [green-blue; $(C_{\text{initial}, j} - C_{\text{minimum}, j})/C_{\text{initial}, j}$] in (%) of the maximum and minimum event concentration in relation to the initial concentration for each event j . Values of 0 indicate that the maximum/minimum concentration is equal to the initial concentration. The black line represents the 1:1 line. The first column, first row and diagonal represent the distribution of the relative concentration increase and decrease for each solute. Upper-right triangle**



500 of sub-figures: For each pair, the correlation coefficients for all points (green-blue plus red) in black as well as for the red or green-blue points in red or green-blue, respectively.



Figure C2: Inter-event synchrony for all 21 solute pairs for Strengbach. See the figure caption of Figure C1 for further explanation.

Data availability

The data supporting the findings of this study are available from the corresponding authors upon reasonable request.



505 **Author contribution**

NB, OF, MCP, SG, HH, ACPW: Conceptualization; NB: Formal analysis; OF, MCP, JG: Funding acquisition; NB, SC, MF, PF, CF, YH, PP, MCP, OF, APCW: Methodology and Investigation; NB: writing – original draft preparation; OF, SG, MCP, ACPW, CF: writing – review and editing.

Competing interests

510 The contact authors have declared that none of the authors has any competing interests.

Disclaimer

xxx

Acknowledgements

The Critex Programme ANR-11-EQPX-0011 funded the Riverlabs and most of the costs associated with their running. The
515 people who run the Riverlabs were staff from ORACLE, OHGE and AgrHyS Critical Zone Observatories (i.e. staff from
CNRS and INRAE). The research units UR HYCAR, IPGP, LHYGES/ITES, UMR SAS and UMR Geosciences Rennes
contributed to the current costs, especially vehicle costs associated with regular travels to the site for maintenance, power
supply, etc. The post-doctoral position of N.B. was co-funded by Region Bretagne, UMR SAS, INRAE (AQUA) and
OZCAR-RI. We thank technical and analytical staff (Beatrice Trinkler, Laure Cordier, Sophie Gangloff, Arnaud Blanchouin,
520 Alain Hernandez, Anthony Julien, Pascal Friedmann) as well as Laurent Ruiz, Rémi Dupas and Chantal Gascuel-Odoux for
inspiring discussions.

References

- 525 Ackerer, J., Jeannot, B., Delay, F., Weill, S., Lucas, Y., Fritz, B., Viville, D., and Chabaux, F.: Crossing hydrological and
geochemical modeling to understand the spatiotemporal variability of water chemistry in a headwater catchment (Strengbach,
France), *Hydrol. Earth Syst. Sci.*, 24, 3111–3133, <https://doi.org/10.5194/hess-24-3111-2020>, 2020.
- Anderson, S., Dietrich, W. E., Torres, R., Montgomery, D. R., and Loague, K.: Concentration-discharge relationships in runoff
from a steep, unchanneled catchment, *Water Resour. Res.*, 33, 211–225, <https://doi.org/10.1029/96WR02715>, 1997.
- Aquilina, L., Poszwa, A., Walter, C., Vergnaud, V., Pierson-Wickmann, A.-C., and Ruiz, L.: Long-Term Effects of High
Nitrogen Loads on Cation and Carbon Riverine Export in Agricultural Catchments, *Environ. Sci. Technol.*, 46, 9447–9455,
530 <https://doi.org/10.1021/es301715t>, 2012.



- Aubert, A. H., Gascuel-Oudou, C., Gruau, G., Akkal, N., Faucheux, M., Fauvel, Y., Grimaldi, C., Hamon, Y., Jaffrézic, A., Lecoz-Boutnik, M., Molénat, J., Petitjean, P., Ruiz, L., and Merot, P.: Solute transport dynamics in small, shallow groundwater-dominated agricultural catchments: insights from a high-frequency, multisolute 10 yr-long monitoring study, *Hydrol. Earth Syst. Sci.*, 17, 1379–1391, <https://doi.org/10.5194/hess-17-1379-2013>, 2013.
- 535 Ávila, A., Piñol, J., Rodà, F., and Neal, C.: Storm solute behaviour in a montane Mediterranean forested catchment, *J. Hydrol.*, 140, 143–161, [https://doi.org/10.1016/0022-1694\(92\)90238-Q](https://doi.org/10.1016/0022-1694(92)90238-Q), 1992.
- Ayraud, V., Aquilina, L., Labasque, T., Pauwels, H., Molenat, J., Pierson-Wickmann, A.-C., Durand, V., Bour, O., Tarits, C., Le Corre, P., Fourre, E., Merot, P., and Davy, P.: Compartmentalization of physical and chemical properties in hard-rock aquifers deduced from chemical and groundwater age analyses, *Appl. Geochem.*, 23, 2686–2707, <https://doi.org/10.1016/j.apgeochem.2008.06.001>, 2008.
- 540 Barthold, F. K., Tyralla, C., Schneider, K., Vaché, K. B., Frede, H.-G., and Breuer, L.: How many tracers do we need for end member mixing analysis (EMMA)? A sensitivity analysis, *Water Resour. Res.*, 47, W08519, <https://doi.org/10.1029/2011WR010604>, 2011.
- Barthold, F. K., Turner, B. L., Elsenbeer, H., and Zimmermann, A.: A hydrochemical approach to quantify the role of return flow in a surface flow-dominated catchment: The role of return flow in a surface flow-dominated catchment, *Hydrol. Process.*, 31, 1018–1033, <https://doi.org/10.1002/hyp.11083>, 2017.
- 545 Beaulieu, E., Pierret, M.-C., Legout, A., Chabaux, F., Goddérís, Y., Viville, D., and Herrmann, A.: Response of a forested catchment over the last 25 years to past acid deposition assessed by biogeochemical cycle modeling (Strengbach, France), *Ecol. Model.*, 430, 109124, <https://doi.org/10.1016/j.ecolmodel.2020.109124>, 2020.
- 550 Bierozza, M., Acharya, S., Benisch, J., ter Borg, R. N., Hallberg, L., Negri, C., Pruitt, A., Pucher, M., Saavedra, F., Staniszewska, K., van't Veen, S. G. M., Vincent, A., Winter, C., Basu, N. B., Jarvie, H. P., and Kirchner, J. W.: Advances in Catchment Science, Hydrochemistry, and Aquatic Ecology Enabled by High-Frequency Water Quality Measurements, *Environ. Sci. Technol.*, 57, 4701–4719, <https://doi.org/10.1021/acs.est.2c07798>, 2023.
- 555 Cenko-Tok, B., Chabaux, F., Lemarchand, D., Schmitt, A.-D., Pierret, M.-C., Viville, D., Bagard, M.-L., and Stille, P.: The impact of water–rock interaction and vegetation on calcium isotope fractionation in soil- and stream waters of a small, forested catchment (the Strengbach case), *Geochim. Cosmochim. Acta*, 73, 2215–2228, <https://doi.org/10.1016/j.gca.2009.01.023>, 2009.
- Christophersen, N. and Hooper, R. P.: Multivariate analysis of stream water chemical data: The use of principal components analysis for the end-member mixing problem, *Water Resour. Res.*, 28, 99–107, <https://doi.org/10.1029/91WR02518>, 1992.
- 560 Christophersen, N., Neal, C., Hooper, R. P., Vogt, R. D., and Andersen, S.: Modelling streamwater chemistry as a mixture of soilwater end-members - a step towards second-generation acidification models, *J. Hydrol.*, 116, 307–320, [https://doi.org/10.1016/0022-1694\(90\)90130-P](https://doi.org/10.1016/0022-1694(90)90130-P), 1990.
- Durand, P. and Juan Torres, J. L.: Solute transfer in agricultural catchments: the interest and limits of mixing models, *J. Hydrol.*, 181, 1–22, [https://doi.org/10.1016/0022-1694\(95\)02922-2](https://doi.org/10.1016/0022-1694(95)02922-2), 1996.
- 565 Evans, C. and Davies, T. D.: Causes of concentration/discharge hysteresis and its potential as a tool for analysis of episode hydrochemistry, *Water Resour. Res.*, 34, 129–137, <https://doi.org/10.1029/97WR01881>, 1998.



- Floury, P., Gaillardet, J., Gayer, E., Bouchez, J., Tallec, G., Ansart, P., Koch, F., Gorge, C., Blanchouin, A., and Roubaty, J.-L.: The potamochemical symphony: new progress in the high-frequency acquisition of stream chemical data, *Hydrol. Earth Syst. Sci.*, 21, 6153–6165, <https://doi.org/10.5194/hess-21-6153-2017>, 2017.
- 570 Fovet, O., Ruiz, L., Gruau, G., Akkal, N., Aquilina, L., Busnot, S., Dupas, R., Durand, P., Fauchoux, M., Fauvel, Y., Fléchar, C., Gilliet, N., Grimaldi, C., Hamon, Y., Jaffrezic, A., Jeanneau, L., Labasque, T., Le Henaff, G., Mérot, P., Molénat, J., Petitjean, P., Pierson-Wickmann, A.-C., Squvidant, H., Viaud, V., Walter, C., and Gascuel-Oudou, C.: AgrHyS: An Observatory of Response Times in Agro-Hydro Systems, *Vadose Zone J.*, 17, 1–16, <https://doi.org/10.2136/vzj2018.04.0066>, 2018.
- 575 Gillet, M., Le Gal La Salle, C., Ayrat, P. A., Khaska, S., Martin, P., and Verdoux, P.: Identification of the contributing area to river discharge during low-flow periods, *Hydrol. Earth Syst. Sci.*, 25, 6261–6281, <https://doi.org/10.5194/hess-25-6261-2021>, 2021.
- Godsey, S. E., Kirchner, J. W., and Clow, D. W.: Concentration-discharge relationships reflect chemostatic characteristics of US catchments, *Hydrol. Process.*, 23, 1844–1864, <https://doi.org/10.1002/hyp.7315>, 2009.
- 580 Hill, A. R.: Base cation chemistry of storm runoff in a forested headwater wetland, *Water Resour. Res.*, 29, 2663–2673, <https://doi.org/10.1029/93WR00758>, 1993.
- Hooper, R. P.: Diagnostic tools for mixing models of stream water chemistry, *Water Resour. Res.*, 39, 1055, <https://doi.org/10.1029/2002WR001528>, 2003.
- 585 Hooper, R. P., Christophersen, N., and Peters, N. E.: Modelling streamwater chemistry as a mixture of soilwater end-members — An application to the Panola Mountain catchment, Georgia, U.S.A., *J. Hydrol.*, 116, 321–343, [https://doi.org/10.1016/0022-1694\(90\)90131-G](https://doi.org/10.1016/0022-1694(90)90131-G), 1990.
- James, A. L. and Roulet, N. T.: Investigating the applicability of end-member mixing analysis (EMMA) across scale: A study of eight small, nested catchments in a temperate forested watershed, *Water Resour. Res.*, 42, W08434, <https://doi.org/10.1029/2005WR004419>, 2006.
- 590 Knapp, J. L. A., von Freyberg, J., Studer, B., Kiewiet, L., and Kirchner, J. W.: Concentration–discharge relationships vary among hydrological events, reflecting differences in event characteristics, *Hydrol. Earth Syst. Sci.*, 24, 2561–2576, <https://doi.org/10.5194/hess-24-2561-2020>, 2020.
- Ladouche, B., Probst, A., Viville, D., Idir, S., Baqué, D., Loubet, M., Probst, J.-L., and Bariac, T.: Hydrograph separation using isotopic, chemical and hydrological approaches (Strengbach catchment, France), *J. Hydrol.*, 242, 255–274, [https://doi.org/10.1016/S0022-1694\(00\)00391-7](https://doi.org/10.1016/S0022-1694(00)00391-7), 2001.
- 595 Lukens, E., Neilson, B. T., Williams, K. H., and Brahney, J.: Evaluation of hydrograph separation techniques with uncertain end-member composition, *Hydrol. Process.*, 36, e14693, <https://doi.org/10.1002/hyp.14693>, 2022.
- Molénat, J., Durand, P., Gascuel-Oudou, C., Davy, P., and Gruau, G.: Mechanisms of Nitrate Transfer from Soil to Stream in an Agricultural Watershed of French Brittany, *Water. Air. Soil Pollut.*, 133, 161–183, <https://doi.org/10.1023/A:1012903626192>, 2002.
- 600 Neal, C., Reynolds, B., Rowland, P., Norris, D., Kirchner, J. W., Neal, M., Sleep, D., Lawlor, A., Woods, C., Thacker, S., Guyatt, H., Vincent, C., Hockenhull, K., Wickham, H., Harman, S., and Armstrong, L.: High-frequency water quality time series in precipitation and streamflow: From fragmentary signals to scientific challenge, *Sci. Total Environ.*, 434, 3–12, <https://doi.org/10.1016/j.scitotenv.2011.10.072>, 2012.



- 605 Pierret, M.-C., Stille, P., Prunier, J., Viville, D., and Chabaux, F.: Chemical and U–Sr isotopic variations in stream and source waters of the Strengbach watershed (Vosges mountains, France), *Hydrol. Earth Syst. Sci.*, 18, 3969–3985, <https://doi.org/10.5194/hess-18-3969-2014>, 2014.
- Pierret, M.-C., Cotel, S., Ackerer, P., Beaulieu, E., Benarioumlil, S., Boucher, M., Boutin, R., Chabaux, F., Delay, F., Fourtet, C., Friedmann, P., Fritz, B., Gangloff, S., Girard, J.-F., Legtchenko, A., Viville, D., Weill, S., and Probst, A.: The Strengbach Catchment: A Multidisciplinary Environmental Sentry for 30 Years, *Vadose Zone J.*, 17, 1–17, <https://doi.org/10.2136/vzj2018.04.0090>, 2018.
- 610 Pierret, M.-C., Viville, D., Dambrine, E., Cotel, S., and Probst, A.: Twenty-five year record of chemicals in open field precipitation and throughfall from a medium-altitude forest catchment (Strengbach - NE France): An obvious response to atmospheric pollution trends, *Atmos. Environ.*, 202, 296–314, <https://doi.org/10.1016/j.atmosenv.2018.12.026>, 2019.
- 615 Pierson-Wickmann, A.-C., Aquilina, L., Martin, C., Ruiz, L., Molénat, J., Jaffrézic, A., and Gascuel-Oudou, C.: High chemical weathering rates in first-order granitic catchments induced by agricultural stress, *Chem. Geol.*, 265, 369–380, <https://doi.org/10.1016/j.chemgeo.2009.04.014>, 2009.
- Rode, M., Wade, A. J., Cohen, M. J., Hensley, R. T., Bowes, M. J., Kirchner, J. W., Arhonditsis, G. B., Jordan, P., Kronvang, B., Halliday, S. J., Skeffington, R. A., Rozemeijer, J. C., Aubert, A. H., Rinke, K., and Jomaa, S.: Sensors in the Stream: The High-Frequency Wave of the Present, *Environ. Sci. Technol.*, 50, 10297–10307, <https://doi.org/10.1021/acs.est.6b02155>, 2016.
- 620 Strohmenger, L., Ackerer, P., Belfort, B., and Pierret, M.-C.: Local and seasonal climate change and its influence on the hydrological cycle in a mountainous forested catchment, *J. Hydrol.*, 610, 127914, <https://doi.org/10.1016/j.jhydrol.2022.127914>, 2022.